Munawwar Mohabuth, Andrei Kotousov, Ching-Tai Ng
Large acoustoelastic effect for Lamb waves propagating in an incompressible elastic plate
Journal of the Acoustical Society of America, 2019; 145(3):1221-1229

Large acoustoelastic effect for Lamb waves propagating in an incompressible elastic plate

Munawwar Mohabuth[a] and Andrei Kotousov
School of Mechanical Engineering, The University of Adelaide, Adelaide, South Australia 5005, Australia

Ching-Tai Ng
School of Civil, Environmental and Mining Engineering, The University of Adelaide, Adelaide, South Australia 5005, Australia

(Received 2 October 2018; revised 4 February 2019; accepted 11 February 2019; published online 5 March 2019)

In this paper, the effect of a large pre-stress on the propagation of small amplitude Lamb waves in an incompressible elastic plate is investigated. Using the theory of incremental elasticity, the dispersion equations, which give the phase velocity of the symmetric and anti-symmetric wave modes as a function of the wavenumber, plate thickness, and pre-stress state, are derived for a general strain energy function. By considering the fourth-order strain energy function of incompressible isotropic elasticity, the correction to the phase velocity due to the pre-stress is obtained implicitly to the second order in the pre-strain/stress, and depends on the second, third, and fourth-order elastic constants. Numerical results are presented to show the dependence of the phase velocity of the Lamb wave modes upon the applied stress. These are compared to the first-order correction, and agree well with the limiting and asymptotic values obtained previously. It is envisaged that the present results may well find important practical applications in various guided wave based ultrasonic techniques utilising gels and rubber-like materials.
https://doi.org/10.1121/1.5092604

[MD] Pages: 1221–1229

I. INTRODUCTION

In recent years, there has been an increased interest in the acoustics of rubber-like solids, as well as soft biological tissues, with the ultimate objective of mastering all aspects of ultrasonic wave techniques. In particular, much research has been directed toward the investigation of the acoustoelastic effect associated with bulk waves (Destrade and Ogden, 2010; Destrade *et al.*, 2010a). Another type of wave motion, which is of great importance in practical applications, is represented by guided waves. Lamb waves, which are guided waves in plate-like structures, are widely utilised in the imaging of defects (Ng, 2015; Aryan *et al.*, 2017) and have many advantages as compared to bulk waves, including a longer propagation range, higher sensitivity to damage, and a lower energy requirement for excitation and sensing (Su and Ye, 2009; Rose, 2014). These advantages are yet to be utilised for soft materials and rubber-like solids. Such materials often exhibit nearly incompressible behaviour and are constrained to undergo essentially volume preserving deformations. At the same time, the strain conditions may reach up to hundreds of percent (Destrade *et al.*, 2010a). Therefore, it is important to understand the effect of these conditions on the wave propagation characteristics; the latter is the focus of the current paper.

The problem of wave propagation in pre-stressed plates has been an active research topic over the past decades. Two approaches have been established for treating this problem, namely, the theory of exact nonlinear elasticity and the theory of weakly nonlinear elasticity. The first approach is amenable to large deformations and has been used to study the behaviour of elastomers and soft solids (Destrade *et al.*, 2010a). In this framework, the strain energy function is written in a general form as a function of the first three principal invariants of the right Cauchy-Green strain tensor (Destrade *et al.*, 2010b). A comprehensive treatment of the foundations of this framework can be found in the pioneering paper by Ogden and Roxburgh (1993). These authors derived dispersion relations for wave propagation in a pre-stressed incompressible finite plate and investigated the vibration and stability phenomena. Since then, there has been a number of contributions on the dynamics of incompressible (Rogerson and Fu, 1995; Rogerson, 1997; Rogerson and Sandiford, 1999; Kaplunov *et al.*, 2000, 2002a,b; Pichugin and Rogerson, 2001, 2002a,b) and compressible (Nolde *et al.*, 2004; Rogerson and Prikazchikova, 2009; Kayestha *et al.*, 2011) pre-stressed plates, focusing on the asymptotic analysis of the dispersion relations.

The second approach, the theory of weakly nonlinear elasticity, is often used in the study of small but not necessarily infinitesimal deformations. In this approach, the strain energy function is generally expanded in terms of the invariants of the Green-Lagrange strain tensor or some other measure of strain (Destrade *et al.*, 2010c). This framework has been employed to describe the acoustoelastic effect, which explains the change in the wave speed with the applied stress. Whilst the theory of acoustoelasticity is well established for bulk waves (Pao *et al.*, 1984; Pao and Gamer, 1985; Guz and Makhort, 2000; Kim and Sachse, 2001),

[a]Electronic mail: munawwar.mohabuth@adelaide.edu.au

comparatively little attention has been given to Lamb waves. An extensive analytical framework was established by Gandhi *et al.* (2012) to analyse the effect of biaxial loading in an initially isotropic compressible plate. Pau and Lanza di Scalea (2015) also developed a nonlinear model to investigate wave propagation in pre-stressed plates. Their model recovers the results of Gandhi *et al.* (2012) in the linearised case but in the nonlinear case, it gives the variation of the amplitude of the second harmonic component as a function of the pre-stress. Other related studies within the weakly nonlinear elasticity framework include Kubrusly *et al.* (2016), Mohabuth *et al.* (2016), Mohabuth *et al.* (2018), Pei and Bond (2016, 2017), Peddeti and Santhanam (2018), and Dubuc *et al.* (2017, 2018).

In all of the abovementioned research set within the theory of weakly nonlinear elasticity, the strain energy function was expanded to the third order in the strain and higher order terms were neglected. The tacit assumption was that the pre-deformation is small, and the correction to the wave speed was obtained implicitly to the first order in the strain and involves second- as well as third-order elastic constants. Motivated by the simplicity of the fourth-order strain energy function of incompressible isotropic elasticity (Hamilton *et al.*, 2004), Destrade *et al.* (2010a) obtained the secular equations for shear wave and surface wave speeds to the second order in the strain for an incompressible solid subjected to a uniaxial pre-stress. Subsequently, Abiza *et al.* (2012) determined the second-order correction to the longitudinal and shear wave speeds for compressible solids in the case of hydrostatic pre-stress and uniaxial pre-stress. These equations involve a combination of the second-, third-, and fourth-order constants and describe the so-called large acoustoelastic effect, which couples the speed of a small amplitude wave to a small-but-finite pre-deformation. These relationships provide a theoretical framework for the experimental determination of third- and fourth-order constants.

The objective of this work is to investigate the large acoustoelastic effect associated with the propagation of Lamb waves in an isotropic incompressible elastic plate. The paper is organised as follows. In Sec. II, the equations governing the propagation of small-amplitude waves in pre-stressed media are briefly reviewed. The dispersion relations for Lamb waves propagating in a pre-stressed plate along a principal direction are then derived in Sec. III for a general form of the strain energy function. The latter is specialised to weakly nonlinear elasticity in Sec. IV by considering the fourth-order strain energy function of incompressible isotropic elasticity, which is applicable to rubber-like materials with large elastic strain limits. It is noted here that the dispersion relations depend on the strain energy function and the pre-stress through the components of the elasticity tensor. In Sec. V, the pre-stress is specialised to the case of a small-but-finite uniaxial pre-deformation along the direction of wave propagation, and the components of the elasticity tensor are expanded up to the second order in the pre-strain. In Sec. VI, the dispersion relations are solved numerically to obtain, implicitly, the second-order correction to the phase velocity due to the pre-stress, i.e., the large acoustoelastic effect. The results are compared to the classical acoustoelastic effect with particular attention to the limiting behaviour of the fundamental and higher order modes in the long and short wave regions.

II. GOVERNING EQUATIONS

In this section, the equations governing the propagation of small amplitude waves in pre-stressed incompressible media are briefly reviewed. These equations are derived based on the theory of incremental motions superimposed a finite deformation. For a comprehensive discussion of the latter theory, the reader is referred to Ogden (1984, 2007). This framework is used in the derivation of dispersion relations for waves propagating in a pre-stressed incompressible plate.

Consider an isotropic hyperelastic incompressible body in some stress-free reference configuration. Suppose the body is subjected to a pure homogeneous finite static deformation such that a material point $\boldsymbol{X}$ in the reference configuration takes up the position $\boldsymbol{x}$ in the deformed configuration. If $\boldsymbol{X}$ and $\boldsymbol{x}$ are referred to the same fixed rectangular Cartesian system of axes, the deformation can be expressed as

$$x_i = \lambda_i X_i, \quad i \in \{1,2,3\}, \tag{1}$$

where the constants λ_i are the principal stretches of the deformation, and the principal axes of the deformation are taken to coincide with the Cartesian coordinate directions. The principal Cauchy stresses required to maintain the body in the static state of deformation are given by

$$\sigma_i = \lambda_i \frac{\partial W}{\partial \lambda_i} - p, \quad i \in \{1,2,3\}, \tag{2}$$

where W is the strain energy function per unit volume and p is a Lagrange multiplier associated with the incompressibility constraint, $\lambda_1\lambda_2\lambda_3 = 1$. The usual summation convention does not apply to Eqs. (1) and (2).

A small-amplitude time dependent motion, given by the mechanical displacement $\boldsymbol{u} = \boldsymbol{u}(\boldsymbol{x}, t)$ where t is time, is then superimposed on the static finite deformation. The mechanical response is described by the incremental constitutive equations (Dowaikh and Ogden, 1990)

$$\hat{\mathrm{S}}_{ij} = \mathcal{A}_{ijkl} u_{l,k} + p u_{i,j} - p^* \delta_{ij}, \quad i,j \in \{1,2,3\}, \tag{3}$$

where $\hat{\mathrm{S}}_{ij}$ is the incremental nominal stress tensor, $\mathcal{A}_{ijkl}$ is the fourth-order elasticity tensor of instantaneous elastic moduli, p^* is the incremental form of p, and a comma indicates partial differentiation with respect to the current coordinates $\boldsymbol{x} \equiv x_i$. The corresponding incremental equations of motion then read

$$\mathcal{A}_{ijkl}\, u_{l,ik} - p^*_{,j} = \rho \ddot{u}_j, \quad i,j \in \{1,2,3\}, \tag{4}$$

where ρ is the density of the material and a superposed dot indicates partial differentiation with respect to time. The coupled incremental incompressibility constraint has the form

$$u_{i,i} = 0, \quad i \in \{1,2,3\}. \tag{5}$$

It is worth noting for later reference that relative to the principal axes of the deformation, the non-zero components of the elasticity tensor are given by

$$\begin{aligned}
&\mathcal{A}_{iijj} = \lambda_i \lambda_j W_{ij}\,,\\
&\mathcal{A}_{ijij} = (\lambda_i W_i - \lambda_j W_j)\,\lambda_i^2/(\lambda_i^2 - \lambda_j^2), \quad i \neq j,\ \lambda_i \neq \lambda_j\\
&\mathcal{A}_{ijij} = (\mathcal{A}_{iiii} - \mathcal{A}_{iijj} + \lambda_i W_i)\,/2, \quad i \neq j,\ \lambda_i = \lambda_j\\
&\mathcal{A}_{ijji} = \mathcal{A}_{jiij} = \mathcal{A}_{ijij} - \lambda_i W_i, \quad i \neq j,
\end{aligned} \tag{6}$$

where $W_{ij} = \partial W/\partial \lambda_i,\ W_{ij} = \partial^2 W/\partial \lambda_i \partial \lambda_j,\ i,j \in \{1,2,3\}$, and there is no sum on repeated indices.

III. DISPERSION RELATIONS

The framework described in Sec. II allows the acoustoelastic effect to be investigated by considering the propagation of small-amplitude homogeneous plane waves in a deformed body. This framework is here extended to study the propagation of Lamb waves in a pre-stressed incompressible plate.

Consider the unstressed body to correspond to a plate of thickness h_0 and infinite lateral extent. Suppose the plate is subjected to a pure homogeneous strain such that its thickness changes to h in the deformed configuration. The Cartesian coordinate system is chosen to be coaxial with the principal axes of the deformation with the origin in the mid-plane of the plate and the x_2 axis normal to the plane of the plate.

In this paper, the analysis is restricted to wave propagation along an in-plane principal direction. For simplicity, the principal direction is taken to be along the x_1 axis, and the analysis is confined to plane incremental motions in the $x_1 - x_2$ plane, with $u_3 = 0$ and u_1 and u_2 taken as independent of x_3. The incremental equations of motion (4) and the incompressibility constraint (5) then reduce to

$$\begin{aligned}
\rho \ddot{u}_1 &= \mathcal{A}_{1111}\, u_{1,11} + (\mathcal{A}_{1122} + \mathcal{A}_{2112}) u_{2,12}\\
&\quad + \mathcal{A}_{2121}\, u_{1,22} - p^*_{,1},\\
\rho \ddot{u}_2 &= \mathcal{A}_{1212}\, u_{2,11} + (\mathcal{A}_{1122} + \mathcal{A}_{2112}) u_{1,12}\\
&\quad + \mathcal{A}_{2222}\, u_{2,22} - p^*_{,2},
\end{aligned} \tag{7}$$

and

$$u_{1,1} + u_{2,2} = 0. \tag{8}$$

The corresponding incremental surface tractions are obtainable from Eq. (3) and can be written explicitly as

$$\begin{aligned}
\hat{S}_{22} &= \mathcal{A}_{2211} u_{1,1} + (\mathcal{A}_{2222} + p) u_{2,2} - p^*,\\
\hat{S}_{21} &= (\mathcal{A}_{2112} + p) u_{2,1} + \mathcal{A}_{2121} u_{1,2}.
\end{aligned} \tag{9}$$

The propagation of acoustoelastic Lamb waves requires the incremental equations of motion to be solved in conjunction with the incompressibility constraint and incremental traction free boundary conditions at the surfaces of the plate, i.e., $\hat{S}_{22} = \hat{S}_{21} = 0$ at $x_2 = \pm\lambda_2 h_0/2 = \pm h/2$. The detailed solution process is rather lengthy and only the final characteristic equations are presented here. These are given by

$$\begin{aligned}
&D_{11} D_{23} \cot(\gamma\alpha_1) - D_{13} D_{21} \cot(\gamma\alpha_3) = 0,\\
&D_{11} D_{23} \tan(\gamma\alpha_1) - D_{13} D_{21} \tan(\gamma\alpha_3) = 0,
\end{aligned} \tag{10}$$

corresponding to the symmetric and anti-symmetric Lamb wave modes, respectively, with $\gamma = kh/2$. These equations form the secular dispersion relations, which provide an implicit relationship between the phase velocity and wavenumber. The definition of the various terms used in the above equations are provided in the Appendix of this paper.

It is worth noting that similar dispersion relations have been derived by Ogden and Roxburgh (1993), albeit their efforts were focused on the effect of the pre-stress on the modes of vibrations of an incompressible finite plate and stability of the underlying deformed configuration.

IV. WEAKLY NONLINEAR ELASTICITY

In the theory of incremental elasticity, the amplitude of the wave motion is assumed to be infinitesimal but no restriction is imposed on the magnitude of the pre-deformation. For small pre-deformations, the strain energy function is often prescribed using the theory of weakly nonlinear elasticity. In this theory, the strain energy function is usually expressed as a power series in terms of the invariants of the Green-Lagrange strain tensor, $\boldsymbol{E}$ (Destrade and Ogden, 2010)

$$I_1 = \operatorname{tr}\boldsymbol{E}, \quad I_2 = \operatorname{tr}\boldsymbol{E}^2, \quad I_3 = \operatorname{tr}\boldsymbol{E}^3. \tag{11}$$

In classical acoustoelasticity, the aim is to determine the first-order corrections to the wave speeds for an infinitesimal pre-strain and thus, the strain energy function is expanded to the third order in the strain. For an incompressible isotropic material, the general weakly nonlinear third-order expansion is given by

$$W = \mu I_2 + \frac{A}{3} I_3, \tag{12}$$

where μ and A are the second- and third-order elasticity constants. In order to study the large acoustoelastic effect for small-but-finite pre-deformations, the strain energy function is truncated at the fourth-order term, and the corrections to the wave speeds are then obtained to the second order in the strain. The general strain energy function of fourth-order incompressible elasticity was recently established by Hamilton *et al.* (2004) and has the form

$$W = \mu I_2 + \frac{A}{3} I_3 + D I_2^2, \tag{13}$$

where D is the so-called fourth-order elastic constant.

The implications of the fourth-order expansion on the acoustoelasticity of shear waves and surface waves was considered by Destrade *et al.* (2010a). These authors derived explicit expressions for the second-order corrections to the wave speeds in the case of a uniaxial pre-stress. Their results show that for "soft" solids it is sufficient to elongate the

material by a few percent to perceive the large acoustoelastic effect. In passing, it should be noted that a fourth-order expansion of the strain energy can also be obtained for compressible isotropic materials, and similar explicit expressions for the corrections to the wave speeds can be derived (see, for example, Abiza *et al.*, 2012). However, fourth-order constants are not readily available for metals and other stiff solids due to yielding and plasticity.

In the present work, a particular form of Hamilton's expansion cast in terms of the principal stretches of the deformation shall be employed

$$W = \frac{\mu}{4}\left[\left(\lambda_1^2-1\right)^2+\left(\lambda_2^2-1\right)^2+\left(\lambda_3^2-1\right)^2\right] + \frac{A}{24}\left[\left(\lambda_1^2-1\right)^3+\left(\lambda_2^2-1\right)^3+\left(\lambda_3^2-1\right)^3\right] + \frac{D}{16}\left[\left(\lambda_1^2-1\right)^2+\left(\lambda_2^2-1\right)^2+\left(\lambda_3^2-1\right)^2\right]^2, \quad (14)$$

in which the connection between the eigenvalues E_i of the Green-Lagrange strain tensor and the principal stretches given by $E_i = (\lambda_i^2 - 1)/2$ has been utilised. It should be noted here that the principal stretches are not independent but are related by the incompressibility condition, $\lambda_1\lambda_2\lambda_3 = 1$.

V. UNIAXIAL PRE-DEFORMATION

In this section, the pre-deformation is specialised to a uniaxial tension in the plane of the plate. It is assumed that the plate has been pre-stressed by the application of a Cauchy stress σ_1 along the x_1 direction such that it is finitely deformed. The elongation in this direction is denoted by $e_1 = \lambda_1 - 1$, where λ_1 is the corresponding axial stretch. Because of symmetry, the lateral stretches in the x_2 and x_3 directions are equal to each other, indicating that the deformation is equi-biaxial. It follows from the incompressibility constraint that the stretch ratios are related by

$$\lambda_3 = \lambda_2 = \lambda_1^{-1/2}. \quad (15)$$

For the specified form of the strain energy function in Eq. (14), the Cauchy stress σ_1 can be computed using Eqs. (2) and (15). The pre-stress can then be expanded in terms of the pre-strain e_1, up to the second order, as (Destrade *et al.*, 2010a)

$$\sigma_1 = 3\mu e_1 + 3\left(\mu + \frac{A}{4}\right)e_1^2. \quad (16)$$

Alternatively, the pre-strain can be expressed in terms of the pre-stress as (Destrade *et al.*, 2010a)

$$e_1 = \frac{1}{3\mu}\sigma_1 - \frac{1}{9\mu^3}\left(\mu + \frac{A}{4}\right)\sigma_1^2. \quad (17)$$

In deriving Eqs. (16) and (17), use has been made of the fact that $p = \lambda_2 W_2$, which is obtained from the condition that the lateral faces are traction free ($\sigma_3 = \sigma_2 = 0$).

The components of the elasticity tensor can similarly be expanded up to the second order in the pre-strain using Eqs. (6), (14), and (15). For brevity, only the non-zero components of the elasticity tensor used in the derivation of the dispersion relations in Eq. (10) are listed here

$$\begin{aligned}
\mathcal{A}_{1111} &= 2\mu + (10\mu + 2A)e_1 + (17\mu + 10A + 14D)e_1^2,\\
\mathcal{A}_{2222} &= 2\mu - (5\mu + A)e_1 + (8\mu + 13A/4 + 8D)e_1^2,\\
\mathcal{A}_{1122} &= -4De_1^2,\\
\mathcal{A}_{1221} &= \mu + (\mu + A/4)e_1 + (3A/4 + 3D)e_1^2,\\
\mathcal{A}_{2121} &= \mu + (A/4)e_1 + (2\mu + A + 3D)e_1^2,\\
\mathcal{A}_{1212} &= \mu + (3\mu + A/4)e_1 + (5\mu + 7A/4 + 3D)e_1^2. \quad (18)
\end{aligned}$$

It is worth noting that the expressions for $\mathcal{A}_{1111}$, $\mathcal{A}_{1212}$, $\mathcal{A}_{2222}$, and $\mathcal{A}_{2121}$ were first obtained by Abiza *et al.* (2012).

For a given uniaxial stress field defined by σ_1 (with $\sigma_3 = \sigma_2 = 0$), the elongation e_1 can be evaluated using Eq. (17) and the components of the elasticity tensor, $\mathcal{A}_{ijkl}$, can then be determined using Eq. (18). Using the latter components, the dispersion relations in Eq. (10) can be solved to obtain, implicitly, the second-order correction to the phase velocity due to the pre-stress.

VI. NUMERICAL RESULTS

The dispersion relations (10) provide an implicit relationship between the phase velocity, wavenumber, plate thickness, and applied stress. These relations can only be solved numerically, and the results are typically presented in the form of dispersion curves, showing the variation of the phase velocity of the Lamb wave modes as a function of the wavenumber-thickness product for different magnitudes of the applied stress. The material considered in this study is silicone rubber, which was selected due to its large elastic strain limit. The elastic properties of this material were obtained from the experimental data of Abiza *et al.* (2012) and are summarised in Table I.

Figure 1 shows the dispersion curves associated with the first three modes of symmetric and anti-symmetric motion for a plate subjected to a uniaxial tension of $\bar{\sigma}_1 = \sigma_1/\mu = 1.37$. The results are here presented in terms of the non-dimensional squared phase velocity $\bar{v} = \rho v^2/\mu$ as a function of the non-dimensional wavenumber $k{\cdot}h_0$. It is emphasised that the thickness of the undeformed plate, h_0, is used here rather than the deformed plate thickness, h, in order to take into account the effect of the applied stress on the phase velocity due to the change in the plate thickness. A semi-log scale is used here to clearly show the behaviour of the different modes in the low and high wavenumber limits. In the long wave region as $k{\cdot}h_0 \to 0$, it can be seen that the fundamental symmetric ($S0$) and anti-symmetric ($A0$) modes have distinct squared phase velocity limits but in the short wave region as $k{\cdot}h_0 \to \infty$, they both approach the same squared phase velocity limit. On the

TABLE I. Elastic properties for silicone rubber.

Parameter	Value (kPa)
$\boldsymbol{\mu}$	109.35
$\boldsymbol{A}$	−454.18
$\boldsymbol{D}$	109.27

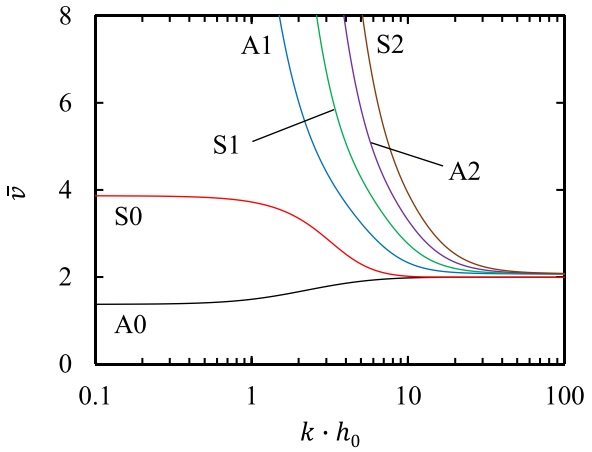

FIG. 1. (Color online) Dispersion curves for the first three symmetric and anti-symmetric modes propagating in an incompressible plate of silicone rubber subjected to a uniaxial tension of $\bar{\sigma}_1 = 1.37$.

other hand, the higher order modes of both the symmetric and anti-symmetric motion have infinite squared phase velocity limits as $k{\cdot}h_0 \to 0$ but they all tend to the same squared phase velocity limit (distinct from that of the fundamental modes) as $k{\cdot}h_0 \to \infty$. These limiting behaviours have been investigated by several researchers who derived appropriate asymptotic expansions (see, for example, Rogerson, 1997). These expansions were used as a means to verify the current approach and numerical results.

The effect of applied stress on the propagation of the different Lamb wave modes is analysed in Fig. 2. The left column shows the variation of the squared phase velocity as a function of the wavenumber-thickness product for different magnitudes of the applied stress. The right column shows the variation of the squared phase velocity as a function of the applied stress for selected values of the wavenumber-thickness product. In both cases, the solid and dashed lines correspond to the large and classical acoustoelastic effects, respectively. The former is concerned with the second-order correction to the squared phase velocity while the latter is concerned with the first-order correction. To obtain the first-order correction, it suffices to keep the linear terms in the expansions (16)–(18) of the stress-strain relation and the components of the elasticity tensor.

The dependence of the fundamental anti-symmetric ($A0$) mode on the applied stress is shown in Fig. 2(a). It is evident that the squared phase velocity increases monotonically with the magnitude of the applied stress. It can also be seen that for compressive stresses the $A0$ mode seems to have specific cutoff values of $k{\cdot}h_0$ below which the wave no longer propagates but are instead growing standing waves (Rogerson and Fu, 1995). These cutoff values depend on the magnitude of $\bar{\sigma}_1$ and correspond to the points at which the curves intersect the axis $\bar{v} = 0$. Below these cutoff values, the phase velocity becomes negative and the underlying deformation becomes unstable for the $A0$ mode (Ogden and Roxburgh, 1993; Rogerson and Fu, 1995). It is also interesting to find that at a pre-stress of $\bar{\sigma}_1 = -1.37$, the classical acoustoelastic formulation predicts that the $A0$ mode does not propagate, whereas the large acoustoelastic formulation predicts otherwise.

In the long wave region as $k{\cdot}h_0 \to 0$, the $A0$ mode is non-dispersive and it can be seen that the curves for both the large and classical acoustoelastic effects tend to the same squared phase velocity limit, equal to the magnitude of the applied stress. This limiting behaviour is found to agree with the asymptotic expansion (63) of Rogerson (1997), which can be shown to reduce, in the present notation, to

$$\bar{v} = \frac{(\mathcal{A}_{1212} - \mathcal{A}_{2121})}{\mu} = \bar{\sigma}_1, \tag{19}$$

in the case when $\sigma_2 = 0$. In the moderate wavenumber regime $(0.1 < k{\cdot}h_0 < 10)$, it can be seen that the solid and dashed lines start to deviate from each other. The deviation is relatively small for lower values of $\bar{\sigma}_1$ but increases at higher values of $\bar{\sigma}_1$, as illustrated in Fig. 2(b). This is not surprising as the contribution of the second-order terms in the expansions (16)–(18) of the stress-strain relation and the components of the elasticity tensor becomes significant at higher values of $\bar{\sigma}_1$. It is worth noting that the $A0$ mode is dispersive in this moderate wavenumber regime and, thus, the squared phase velocity is also dependent on the wavenumber-thickness product. The deviation is found to be relatively small at lower values of $k{\cdot}h_0$ but increases at higher values of $k{\cdot}h_0$, as shown in Fig. 2(b). The variation of $\bar{v}$ with $\bar{\sigma}_1$ is approximately quadratic in the case of the large acoustoelastic effect while an approximately linear trend is observed in the case of the classical acoustoelastic effect. In the short wave region as $k{\cdot}h_0 \to \infty$, the curves for the large and classical acoustoelastic effects converge to different constant values of $\bar{v}$, except at low magnitudes of $\bar{\sigma}_1$ where the solid and dashed lines effectively overlap each other. The limiting squared phase velocities correspond to the squared phase velocities of the associated Rayleigh surface waves (Rogerson, 1997). The secular equation for the surface wave limit was obtained in terms of the elongation by Destrade *et al.* (2010a)

$$\bar{v} = \frac{0.9126\mu + (3\mu + 0.9126A/4)e_1 + (5.642\mu + 2.071A + 3.554D)e_1^2}{\mu}, \tag{20}$$

in the case when $\sigma_2 = 0$. As the $A0$ mode is largely non-dispersive in the high wavenumber regime, the difference in $\bar{v}$ is attributed to the contribution of the second-order terms in the expansions (16)–(18). The latter contribution also helps to explain the quadratic variation of $\bar{v}$ with $\bar{\sigma}_1$ in the case of the large acoustoelastic effect as opposed to the

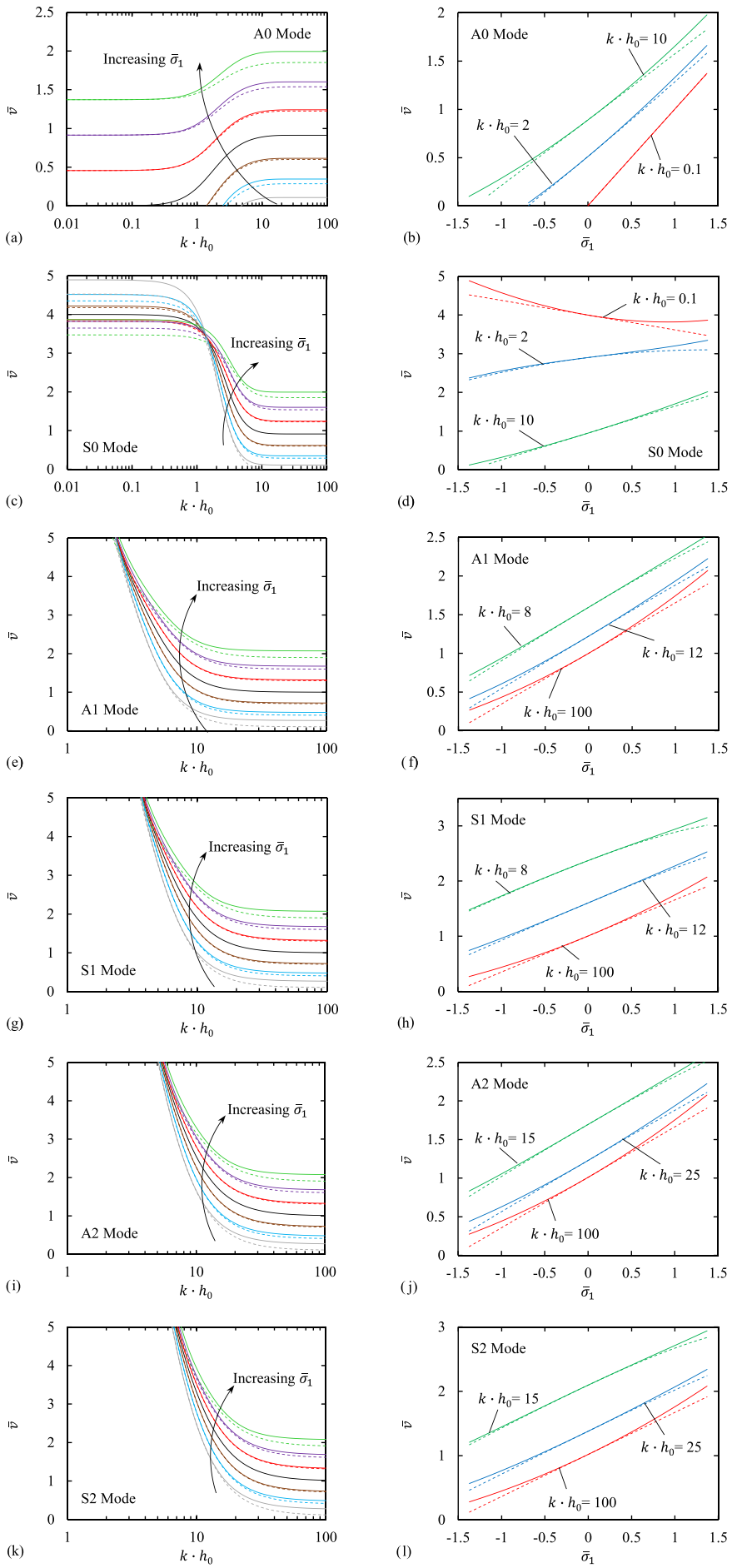

FIG. 2. (Color online) Effect of the applied uniaxial stress on the propagation of Lamb waves in an incompressible layer of silicone rubber. (Left column) Variation of the squared phase velocity as a function of the wavenumber-thickness product for different magnitudes of the applied stress $\bar{\sigma}_1 = \{-1.37, -0.91, -0.46, 0, 0.46, 0.91, 1.37\}$. (Right column) Variation of the squared phase velocity as a function of the applied stress for selected values of the wavenumber-thickness product. (a),(b) *A*0 mode; (c),(d) S0 mode; (e),(f) *A*1 mode; (g),(h) S1 mode; (i),(j) *A*2 mode; and (k),(l) *S*2 mode. The solid (dashed) lines correspond to the large (small) acoustoelastic effects.

linear variation of $\bar{v}$ with $\bar{\sigma}_1$ in the case of the classical acoustoelastic effect.

Figure 2(c) shows the variation of the squared phase velocity of the fundamental symmetric ($S0$) mode with the applied stress. It can be seen that at large values of compressive stress ($\bar{\sigma}_1 < -1.37$), the $S0$ mode seems to have a cutoff value of $k{\cdot}h_0$ above which the wave does not propagate. Similar to the behaviour of the $A0$ mode, the cutoff value of $k{\cdot}h_0$ corresponds to the point at which the deformation becomes unstable for this particular mode. It is also interesting to find that at a pre-stress of $\bar{\sigma}_1 = -1.37$, the classical acoustoelastic formulation predicts that the $S0$ mode ceases to propagate above $k{\cdot}h_0 \sim 10$, whereas the large acoustoelastic formulation shows that the $S0$ mode propagates across the whole spectrum.

In the long wave region as $k{\cdot}h_0 \to 0$, it can be seen that $\bar{v}$ decreases linearly with $\bar{\sigma}_1$ in the case of the classical acoustoelastic effect. However, a nonlinear (quadratic) trend is observed in the case of the large acoustoelastic effect, with $\bar{v}$ decreasing at lower magnitudes of $\bar{\sigma}_1$ but increasing at higher magnitudes of $\bar{\sigma}_1$, as shown in Fig. 2(d). This nonlinear behaviour is found to be in good agreement with the asymptotic expansion (45) obtained by Rogerson (1997), which can be shown to reduce, in the present notation, to

$$\bar{v} = \frac{4\mu + (3\mu + A)e_1 + (29\mu + 55A/4 + 30D)e_1^2}{\mu}, \quad (21)$$

in the case when $\sigma_2 = 0$. The latter equation indicates that the nonlinear behaviour is due to the second-order terms in the expansions (16)–(18), which is not surprising as the $S0$ mode is largely non-dispersive in the low wavenumber regime. In the moderate wavenumber regime ($0.1 < k{\cdot}h_0 < 10$), the $S0$ mode is highly dispersive and, thus, the squared phase velocity is not only dependent on the applied stress but is also a function of the wavenumber-thickness product. As a result, the variation of $\bar{v}$ with $\bar{\sigma}_1$ is nonlinear for both the large (approximately cubic) and classical (approximately quadratic) acoustoelastic effects, as shown in Fig. 2(d). In the short wave region as $k{\cdot}h_0 \to \infty$, the behaviour of the $S0$ mode is the same as that of the $A0$ mode with the limiting squared phase velocities equal to the associated Rayleigh surface wave velocities. The applied stress causes an increase in the squared phase velocity with $\bar{v}$ varying linearly with $\bar{\sigma}_1$ in the case of the classical acoustoelastic effect as compared to a quadratic increase in the case of the large acoustoelastic effect. The quadratic variation is, as discussed earlier, due to the contribution of second-order terms in the expansions (16)–(18) as the $S0$ mode is largely non-dispersive in the high wavenumber regime.

In Figs. 2(e)–2(l), the first two higher order modes of symmetric and anti-symmetric motion are presented. It can be seen that these modes behave in a similar way and have infinite squared phase velocity limits in the long wave region as $k{\cdot}h_0 \to 0$. The higher order modes are all highly dispersive in the low and moderate wavenumber regimes and, hence, the squared phase velocity is dependent on the applied stress as well as on the wavenumber-thickness product. In the moderate wavenumber regime, the squared phase velocity is found to increase monotonically with the applied stress. The variation of $\bar{v}$ with $\bar{\sigma}_1$ is approximately linear for the large acoustoelastic effect, whereas an approximately quadratic variation is observed for the classical acoustoelastic effect. However, the opposite trend is seen in the high wavenumber regime; the large acoustoelastic effect predicts a quadratic dependence of $\bar{v}$ on $\bar{\sigma}_1$ while the classical acoustoelastic effect predicts a linear dependence. This behaviour is expected as in the short wave region as $k{\cdot}h_0 \to \infty$, the higher order modes are largely non-dispersive and converge to the same squared phase velocity limit corresponding to that of a shear wave propagating along the x_1 direction (Rogerson, 1997). The squared phase velocity limit is given by $\bar{v} = \mathcal{A}_{1212}/\mu$, where the expression for $\mathcal{A}_{1212}$ is obtained from the expansions in Eq. (18). At low magnitudes of the applied stress, the curves for the large and classical acoustoelastic effects overlap as the contribution of the second-order terms is relatively small. However, at higher magnitudes of the applied stress, the contribution of the second-order terms is significant, leading to a quadratic increase in the squared phase velocity.

Overall, the wavenumber-thickness range of $k{\cdot}h_0 > 20$ and the applied stress range of $\bar{\sigma}_1 > 0.5$ represent a region of practical interest with respect to the experimental determination of the fourth-order constants using guided waves. In general, fourth-order constants cannot be evaluated using these results for metals and other ordinary elastic solids because of yielding and plasticity. However, for soft solids such as silicone rubber, an elongation of about 15% (corresponding to $\bar{\sigma}_1 = 0.5$) seems to be sufficient to reveal the large acoustoelastic effect. This behaviour is in good agreement with the results of Abiza *et al*. (2012) who showed that an elongation of about 20% is sufficient to evaluate the fourth-order constants experimentally using bulk shear waves.

It is also interesting to compare the results presented here for silicone rubber to those obtained for metals. Several studies have shown that, in the case of aluminum, tensile stresses cause a decrease in the phase velocity of the different Lamb wave modes for wave propagation along the direction of the applied load (Pau and Lanza di Scalea, 2015; Pei and Bond, 2017), which is consistent with the results of bulk wave acoustoelasticity (Hughes and Kelly, 1953). In contrast, the results obtained for silicone rubber show that tensile stresses lead to an increase in the phase velocity of the different modes, apart from the $S0$ mode in the long wave region. This opposing behaviour is a consequence of the values of the higher order elastic constants, which are of the same order of magnitude as the second-order constants for silicone rubber.

VII. CONCLUSION

The classical acoustoelastic theory allows the determination of third-order elastic constants and the evaluation of applied stresses in ordinary elastic materials using bulk waves. However, this theory can produce large discrepancies in the case of relatively soft tissues and rubber-like materials, which are often subjected to high strains. These discrepancies can become quite pronounced in the case of guided

waves as the phase velocities of the different wave modes are dependent on the applied stress as well as the wavenumber-thickness product.

This paper aimed at uncovering the acoustoelastic effect associated with the propagation of small-amplitude Lamb waves in incompressible plate-like structures subjected to a large pre-stress. A new acoustoelastic formulation based on a fourth-order strain energy function was developed to study the effect of a large applied uniaxial stress on the squared phase velocity of the different Lamb wave modes. Dispersion results were presented for a silicone rubber plate and compared with the results obtained using the classical acoustoelastic formulation. At lower magnitudes of the applied stress, the deviation between the large and classical acoustoelastic formulations was found to be relatively small. However, the difference was found to be quite significant at higher magnitudes of the applied stress, showing that the large acoustoelastic formulation should be considered when evaluating the stress in rubber-like materials subjected to high strains.

In general, this paper provides useful analytical benchmarks for experimental studies and the development of guided wave based ultrasonic techniques for soft tissues and rubber-like materials. The presented results can also be easily generalised, for example, to torsional or interfacial waves. Although the framework developed can be extended to compressible materials, the lack of fourth-order elastic constants coupled with the low elastic strain limit of ordinary stiff materials makes this option less attractive.

ACKNOWLEDGMENTS

This work was supported by the Australian Research Council through Discovery Project No. DP160102233. M.M. also gratefully acknowledges the support of the Australian Government Research Training Program Scholarship.

APPENDIX

Following the work of Mohabuth *et al.* (2016), the propagation of homogeneous plane waves in the form

$$\{u_j,\, p^*\} = \{U_j, kP\} e^{ik(x_1+\alpha x_2-ct)}, \quad j \in \{1,2\} \tag{A1}$$

is considered, where U_j is the amplitude of the displacement, P is a scalar, k is the wavenumber along the x_1 direction, α is the ratio of the wavenumbers in the x_2 direction to that in the x_1 direction, and c is the phase velocity in the x_1 direction.

Substituting solutions of this form into Eqs. (7) and (8) yields

$$\begin{aligned}
&\rho U_1 c^2 - \mathcal{A}_{1111}\, U_1 - (\mathcal{A}_{1122} + \mathcal{A}_{2112}) U_2 \alpha \\
&\quad - \mathcal{A}_{2121}\, U_1 \alpha^2 - iP = 0, \\
&\rho U_2 c^2 - \mathcal{A}_{1212}\, U_2 - (\mathcal{A}_{1122} + \mathcal{A}_{2112}) U_1 \alpha \\
&\quad - \mathcal{A}_{2222}\, U_2 \alpha^2 - i\alpha P = 0,
\end{aligned} \tag{A2}$$

and

$$U_1 + U_2 \alpha = 0. \tag{A3}$$

Using the incompressibility constraint (A3) to eliminate U_2 in favour of U_1 in the equations of motion (A2), two homogeneous equations are obtained

$$\begin{aligned}
&U_1(\rho c^2 - \mathcal{A}_{1111} + \mathcal{A}_{1122} + \mathcal{A}_{2112} - \mathcal{A}_{2121}\, \alpha^2) - iP = 0, \\
&U_1(-\rho c^2 + \mathcal{A}_{1212} + (\mathcal{A}_{2222} - \mathcal{A}_{1122} - \mathcal{A}_{2112})\alpha^2) \\
&\quad - i\alpha^2 P = 0.
\end{aligned} \tag{A4}$$

These can be shown to have a non-trivial solution provided that

$$\Lambda_4\, \alpha^4 + \Lambda_2\, \alpha^2 + \Lambda_0 = 0\,, \tag{A5}$$

where

$$\begin{aligned}
\Lambda_4 &= \mathcal{A}_{2121}, \\
\Lambda_2 &= \mathcal{A}_{1111} + \mathcal{A}_{2222} - 2\mathcal{A}_{1122} - 2\mathcal{A}_{2112} - \rho c^2, \\
\Lambda_0 &= \mathcal{A}_{1212} - \rho c^2.
\end{aligned} \tag{A6}$$

The lack of odd power coefficients in Eq. (A5) means that the fourth-order equation can be reduced to a quadratic equation in α^2. This simplification yields four solutions for α, which are denoted by α_q, $q \in \{1,2,3,4\}$, with the following properties:

$$\alpha_2 = -\alpha_1, \quad \alpha_4 = -\alpha_3. \tag{A7}$$

The general solution for u_j and p^* may be expressed as a linear combination of the four linearly independent solutions

$$\{u_1, u_2, p^*\} = \sum_{q=1}^{4} \{1, V_q, kW_q\}\, U_{1q}\, e^{ik(x_1+\alpha_q x_2-ct)}, \tag{A8}$$

where $V_q = U_{2q}/U_{1q}$ and $W_q = P_q/U_{1q}$. These ratios are given by

$$\begin{aligned}
V_q &= -1/\alpha_q, \\
W_q &= -i(\rho c^2 - \mathcal{A}_{1111} + \mathcal{A}_{1122} + \mathcal{A}_{2112} - \mathcal{A}_{2121}\, \alpha_q^2),
\end{aligned} \tag{A9}$$

which are obtained using the relations in Eqs. (A3) and (A4), respectively.

Explicit expressions for the incremental surface tractions may then be found by substituting Eq. (A8) into Eq. (9)

$$\begin{aligned}
\hat{S}_{22} &= \sum_{q=1}^{4} ikD_{1q} U_{1q}\, e^{ik(x_1+\alpha_q x_2-ct)}, \\
\hat{S}_{21} &= \sum_{q=1}^{4} ikD_{2q} U_{1q}\, e^{ik(x_1+\alpha_q x_2-ct)},
\end{aligned} \tag{A10}$$

where

$$\begin{aligned}
D_{1q} &= \rho c^2 - \mathcal{A}_{1111} - \mathcal{A}_{2222} + 2\mathcal{A}_{2112} + 2\mathcal{A}_{1122} \\
&\quad - \mathcal{A}_{2121} - \mathcal{A}_{2121}\alpha_q^2 + \sigma_2, \\
D_{2q} &= \mathcal{A}_{2121}\alpha_q - \mathcal{A}_{2121}/\alpha_q + \sigma_2/\alpha_q.
\end{aligned} \tag{A11}$$

It is noted that in deriving the above expressions, use has been made of the fact that $p = \mathcal{A}_{2121} - \mathcal{A}_{2112} - \sigma_2$ (Ogden, 1984).

The dispersion relations are obtained by imposing incremental traction free boundary conditions on the upper and lower free surfaces of the plate, namely, $\hat{S}_{22} = \hat{S}_{21} = 0$ at $x_2 = \pm\lambda_2 h_0/2 = \pm h/2$. This yields a homogeneous system of four equations, which can be expressed as

$$i\xi \begin{pmatrix} D_{11}E_1 & D_{12}E_2 & D_{13}E_3 & D_{14}E_4 \\ D_{21}E_1 & D_{22}E_2 & D_{23}E_3 & D_{24}E_4 \\ D_{11}\overline{E_1} & D_{12}\overline{E_2} & D_{13}\overline{E_3} & D_{14}\overline{E_4} \\ D_{21}\overline{E_1} & D_{22}\overline{E_2} & D_{23}\overline{E_3} & D_{24}\overline{E_4} \end{pmatrix} \times \begin{pmatrix} U_{11} \\ U_{12} \\ U_{13} \\ U_{14} \end{pmatrix} e^{ik(x_1 - ct)} = \begin{Bmatrix} 0 \\ 0 \\ 0 \\ 0 \end{Bmatrix}, \tag{A12}$$

where $E_q = e^{ik\alpha_q h/2}$ and $\overline{E_q} = e^{-ik\alpha_q h/2}$. For non-trivial solutions, the determinant of the coefficient matrix in Eq. (A12) is set to zero. After some algebra, the determinant can be reduced to two characteristic equations

$$\begin{aligned} &D_{11}D_{23}\cot(\gamma\alpha_1) - D_{13}D_{21}\cot(\gamma\alpha_3) = 0, \\ &D_{11}D_{23}\tan(\gamma\alpha_1) - D_{13}D_{21}\tan(\gamma\alpha_3) = 0, \end{aligned} \tag{A13}$$

corresponding to the symmetric and anti-symmetric Lamb wave modes, respectively, with $\gamma = k{\cdot}h/2$.

Abiza, Z., Destrade, M., and Ogden, R. W. (**2012**). "Large acoustoelastic effect," Wave Motion **49**, 364–374.

Aryan, P., Kotousov, A., Ng, C. T., and Cazzolato, B. S. (**2017**). "A baseline-free and non-contact method for detection and imaging of structural damage using 3D laser vibrometry," Struct. Control Health Monit. **24**, e1894.

Destrade, M., Gilchrist, M. D., and Saccomandi, G. (**2010a**). "Third- and fourth-order constants of incompressible soft solids and the acousto-elastic effect," J. Acoust. Soc. Am. **127**, 2759–2763.

Destrade, M., Gilchrist, M. D., and Ogden, R. W. (**2010b**). "Third- and fourth-order elasticities of biological soft tissues," J. Acoust. Soc. Am. **127**, 2103–2106.

Destrade, M., Gilchrist, M. D., and Murphy, J. G. (**2010c**). "Onset of nonlinearity in the elastic bending of blocks," J. Appl. Mech. **77**(6), 061015.

Destrade, M., and Ogden, R. W. (**2010**). "On the third- and fourth-order constants of incompressible isotropic elasticity," J. Acoust. Soc. Am. **128**, 3334–3343.

Dowaikh, M. A., and Ogden, R. W. (**1990**). "On surface waves and deformations in a pre-stressed incompressible elastic solid," IMA J. Appl. Math. **44**, 261–284.

Dubuc, B., Ebrahimkhanlou, A., and Salamone, S. (**2017**). "The effect of applied stress on the phase and group velocity of guided waves in anisotropic plates," J. Acoust. Soc. Am. **142**, 3553–3563.

Dubuc, B., Ebrahimkhanlou, A., and Salamone, S. (**2018**). "Computation of propagating and non-propagating guided modes in nonuniformly stressed plates using spectral methods," J. Acoust. Soc. Am. **143**, 3220–3230.

Gandhi, N., Michaels, J. E., and Lee, S. J. (**2012**). "Acoustoelastic Lamb wave propagation in biaxially stressed plates," J. Acoust. Soc. Am. **132**, 1284–1293.

Guz, A. N., and Makhort, F. G. (**2000**). "The physical fundamentals of the ultrasonic nondestructive stress analysis of solids," Int. Appl. Mech. **36**(9), 1119–1149.

Hamilton, M. F., Ilinskii, Y. A., and Zabolotskaya, E. A. (**2004**). "Separation of compressibility and shear deformation in the elastic energy density," J. Acoust. Soc. Am. **116**, 41–44.

Hughes, D. S., and Kelly, J. L. (**1953**). "Second-order elastic deformation of solids," Phys. Rev. **92**, 1145–1149.

Kaplunov, J. D., Nolde, E. V., and Rogerson, G. A. (**2000**). "A low-frequency model for dynamic motion in pre-stressed incompressible elastic structures," Proc. R. Soc. Lond. A **456**, 2589–2610.

Kaplunov, J. D., Nolde, E. V., and Rogerson, G. A. (**2002a**). "An asymptotically consistent model for long-wave high-frequency motion in a pre-stressed elastic plate," Math. Mech. Solids **7**(6), 581–606.

Kaplunov, J. D., Nolde, E. V., and Rogerson, G. A. (**2002b**). "Short wave motion in a pre-stressed incompressible elastic plate," IMA J. Appl. Math. **67**, 383–399.

Kayestha, P., Wijeyewickrema, A. C., and Kishimoto, K. (**2011**). "Wave propagation along a non-principal direction in a compressible pre-stressed elastic layer," Int. J. Solids Struct. **48**, 2141–2153.

Kim, K. Y., and Sachse, W. (**2001**). "Acoustoelasticity of elastic solids," in *Handbook of Elastic Properties of Solids, Liquids, and Gases*, edited by A. G. Avery and W. Sachse (Academic, San Diego), Vol. 1, pp. 441–468.

Kubrusly, A. C., Braga, A. M. B., and Von der Weid, J. P. (**2016**). "Derivation of acoustoelastic Lamb wave dispersion curves in anisotropic plates at the initial and natural frames of reference," J. Acoust. Soc. Am. **140**, 2412–2417.

Mohabuth, M., Kotousov, A., and Ng, C.-T. (**2016**). "Effect of uniaxial stress on the propagation of higher-order Lamb wave modes," Int. J. Nonlinear Mech. **86**, 104–111.

Mohabuth, M., Kotousov, A., Ng, C.-T., and Rose, L. R. F. (**2018**). "Implication of changing loading conditions on structural health monitoring utilising guided waves," Smart Mater. Struct. **27**, 025003.

Ng, C. T. (**2015**). "A two-stage approach for quantitative damage imaging in metallic plates using Lamb waves," Earthquakes Struct. **8**, 821–841.

Nolde, E. V., Prikazchikova, L. A., and Rogerson, G. A. (**2004**). "Dispersion of small amplitude waves in a pre-stressed, compressible elastic plate," J. Elasticity **75**, 1–29.

Ogden, R. W. (**1984**). *Non-Linear Elastic Deformations* (Ellis Horwood, Chichester).

Ogden, R. W. (**2007**). "Incremental statics and dynamics of pre-stressed elastic materials," in *Waves in Nonlinear Pre-Stressed Materials*, edited by M. Destrade and G. Saccomandi (Springer, Vienna), Vol. 495, pp. 1–26.

Ogden, R. W., and Roxburgh, D. G. (**1993**). "The effect of pre-stress on the vibration and stability of elastic plates," Int. J. Eng. Sci. **31**(12), 1611–1639.

Pao, Y.-H., and Gamer, U. (**1985**). "Acoustoelastic waves in orthotropic media," J. Acoust. Soc. Am. **77**, 806–812.

Pao, Y.-H., Sachse, W., and Fukuoka, H. (**1984**). "Acoustoelasticity and ultrasonic measurements of residual stresses," in *Physical Acoustics*, edited by W. P. Mason and R. N. Thurston (Academic, New York), Vol. 17, pp. 61–143.

Pau, A., and Lanza di Scalea, F. (**2015**). "Nonlinear guided wave propagation in prestressed plates," J. Acoust. Soc. Am. **137**, 1529–1540.

Peddeti, K., and Santhanam, S. (**2018**). "Dispersion curves for Lamb wave propagation in prestressed plates using a semi-analytical finite element analysis," J. Acoust. Soc. Am. **143**, 829–840.

Pei, N., and Bond, L. (**2016**). "Higher order acoustoelastic Lamb wave propagation in stressed plates," J. Acoust. Soc. Am. **140**, 3834–3843.

Pei, N., and Bond, L. (**2017**). "Comparison of acoustoelastic Lamb wave propagation in stressed plates for different measurement orientations," J. Acoust. Soc. Am. **142**, EL327–EL331.

Pichugin, A. V., and Rogerson, G. A. (**2001**). "A two-dimensional model for extensional motion of a pre-stressed incompressible elastic layer near cut-off frequencies," IMA J. Appl. Math. **66**, 357–385.

Pichugin, A. V., and Rogerson, G. A. (**2002a**). "An asymptotic membrane-like theory for long wave motion in a pre-stressed elastic plate," Proc. R. Soc. Lond. A **458**, 1447–1468.

Pichugin, A. V., and Rogerson, G. A. (**2002b**). "Anti-symmetric motion of a pre-stressed incompressible elastic layer near shear resonance," J. Eng. Math. **42**, 181–202.

Rogerson, G. A. (**1997**). "Some asymptotic expansions of the dispersion relation for an incompressible elastic plate," Int. J. Solids Struct. **34**(22), 2785–2802.

Rogerson, G. A., and Fu, Y. B. (**1995**). "An asymptotic analysis of the dispersion relation of a pre-stressed incompressible elastic plate," Acta Mech. **111**, 59–74.

Rogerson, G. A., and Prikazchikova, L. A. (**2009**). "Generalisations of long wave theories for pre-stressed compressible elastic plates," Int. J. Non-Linear Mech. **44**, 520–529.

Rogerson, G. A., and Sandiford, K. J. (**1999**). "Harmonic wave propagation along a non-principal direction in a pre-stressed elastic plate," Int. J. Eng. Sci. **37**(13), 1663–1691.

Rose, J. (**2014**). *Ultrasonic Guided Waves in Solid Media* (Cambridge University Press, Cambridge).

Su, Z., and Ye, L. (**2009**). "Identification of damage using Lamb waves: From fundamentals to applications," in *Lecture Notes in Applied and Computational Mechanics*, edited by F. Pfeiffer and P. Wriggers (Springer, Berlin).